**Original Article**
**Running Title**: Patuletin: The Anti-Non-Small Lung Cancer Flavonoid
Received: July 14, 2025; Accepted: September 6, 2025

# Patuletin Caused Growth Inhibition of NCI-H460 Cancer Cells via Induction of Apoptosis

Sana Irshad[*], MBBS/MPhil, Hazar Khan[**], MBBS/MPhil, Asma Khawer[*], MBBS/MPhil, Muhammad Aitmaud Uddolah Khan[***], MBBS/MPhil, Anum Razzak[*], MBBS/MPhil, Mudassar, Azhar[****], Pharm.D/PhD, Talat Roome[*], PhD, Shaheen Faizi[*****], PhD, Ahsana Dar Farooq[******], PhD, Muhammad Kashif [*♦], MBBS/PhD

[*]*Department of Pharmacology, Dow University of Health Sciences, Karachi, Pakistan*
[**]*Department of Pharmacology, Makran Medical College, Turbat, Pakistan*
[***]*Department of Pharmacology, Liaquat National Medical College, Karachi, Pakistan*
[****]*Department of Basic Medical Sciences, Salim Habib University, Karachi, Pakistan*
[*****]*International Center for Chemical and Biological Sciences, University of Karachi, Karachi, Pakistan*
[******]*Hamdard Al-Majeed College of Eastern Medicine, Hamdard University, Karachi, Pakistan*

**♦Corresponding Author**
Muhammad Kashif, MBBS/PhD
Department of Pharmacology,
Dow Medical College,
Dow University of Health Sciences,
Karachi, Pakistan
Email: mohd.kashif@duhs.edu.pk

## Abstract

**Background:** Non-small cell lung cancer is among the major causes of mortality, globally. Previous studies demonstrated therapeutic potential of *Tagetes patula* flower methanolic extract against this cancer. The present study aimed at evaluating the anti-cancer potential of patuletin, a flavonoid believed to underlie medicinal effects of Tagetes flower.

**Method:** This experimental study was performed on NCI-H460 cell lines. The cell viability was assessed using Sulforhodamine B assay followed by flow-cytometry-based cell cycle analysis (propidium iodide), assessment of apoptosis [mitochondrial membrane potential and Terminal deoxynucleotidyl transferase dUTP nick end labeling (TUNEL) fluorescence], and deoxyribonucleic acid [DNA (plasmid and genomic)] fragmentation. The expression of BAK, BCL-XL and p53 genes were assessed using quantitative polymerase chain reaction. The doxorubicin served as standard drug. Statistical analysis (One-way ANOVA followed by Least Significant Difference) was performed using SPSS software (v19.0, Chicago, IL, USA). The level of significance was set at $^{*}(P < 0.05)$, $^{**}(P < 0.01)$, and $^{***}(P < 0.005)$.

**Results:** Patuletin arrested the growth of NCI-H460 cells with a 50% growth inhibition ($GI_{50}$) of 61 µg/mL. The cell cycle analysis revealed a significant increase in $G_o/G_1$ and S phases, while $G_2$/M phase demonstrated a decline. The apoptotic index exhibited significant elevation, while

DNA remained intact. The expression of all tested genes was altered, but BAK exhibited remarkable upregulation.
**Conclusion:** Patuletin caused growth inhibition of NCI-H460 via the induction of BAK-mediated apoptosis. Therefore, it presents itself as a promising candidate for anti-non-small cell lung cancer drug discovery program.

***Keywords:*** Carcinoma, Non-small-cell lung, Apoptosis, Antineoplastic agents

## Introduction

Cancer, an abnormal and uncontrolled proliferation of cells, is among the major causes of mortality, worldwide. It is the primary cause of clinical, social and economic burden to humanity with lifetime risk of 20%.[1] Among all various types, lung cancer is the second most prevalent type (after prostate and breast cancer) in both males and females, respectively. It has accounted for 2.8 million diagnoses and 1.8 million deaths with a lifetime risk of 3.8% and 1.77% for men and women, respectively.[2] Tobacco smoking was found to be the primary underlying cause in 80% of the cases.[3] Based on the cell of origin, lung cancer is divided into small cell and non-small cell lung cancers, with later being the most prevalent and malignant due to high metastasis potential.[4] The prevalence of cancer in Pakistan is steadily increasing, including lung cancer, which is currently the 2$^{nd}$ leading cause of cancer in males.[5]

The treatment of non-small cell lung cancer involves surgery, radiotherapy, chemotherapy, immunotherapy and molecular therapy. They are either administered alone or in combination depending upon the stage and complexity of disease.[6] However, prognosis is poor. It is often diagnosed at an advanced stage with a five-year survival rate of less than 5%.[7] Therefore, there is a need to look for newer options for the management of lung cancer. In this regard, it is worth mentioning that humans are blessed with the wealth of natural flora and fauna. They are the rich source of diverse chemical compounds of medicinal value, which have played an instrumental role in the drug discovery process. An estimated 60% of anti-cancer drugs used clinically these days are of natural origin.[8]

Apoptosis, or programmed cell death, is an essential biological process that ensures tissue homeostasis by removing damaged, abnormal, or aged cells. In lung cancer, however, apoptotic pathways are frequently suppressed, allowing malignant cells to evade elimination, continue proliferating, and accumulate genetic alterations. This impairment not only drives tumor progression but also plays a pivotal role in the development of resistance to anticancer therapies.[9] In recent years, restoring apoptosis is recognized as a promising therapeutic strategy to overcome drug resistance in lung cancer. This requires a comprehensive understanding of the molecular regulators of apoptosis and their dysregulation in tumor biology. The p53 and the B-cell lymphoma 2 (BCL2) family [BCL2 Antagonist/Killer (BAK) and B-cell lymphoma-extra large (BCL-XL) have been reported to play a pivotal role in the pathogenesis of lung cancer.[10] The activator BAK, a pro-apoptotic protein, was shown to exert beneficial action against lung cancer.[11] Thus, the strategies aimed at restoring their normal function holds significant therapeutic promise.

*Tagetes patula* (common name = French Marigold) is an edible plant,[12] traditionally used for the management of colics, diarrhea, vomiting, fever, skin, and hepatic diseases.[13, 14] It is of note that traditional

healers has been using its petals for the treatment of cancers.[15] Patuletin is a flavonoid, which is considered to be the major therapeutic moiety residing in Tagetes flower.[16] It was shown to be effective against many cancers such as cervical adenocarcinoma,[17] breast cancer[18] and lung adenocarcinoma.[19] However, its effectiveness is yet to be assessed against the non-small cell lung carcinoma. Keeping this into account, the present study aimed to evaluate the effectiveness of patuletin against lung cancer and shed lights on the potential mechanism of anti-cancer action.

## Materials and Methods

### *Materials*

Following chemicals were used in this study: Bleomycin sulphate, dimethyl sulfoxide (DMSO), fetal bovine serum (FBS), L-glutamine penicillin streptomycin solution (GPSS), poly-D-lysine, propidium iodide, Rosewell park memorial institute (RPMI-1640) medium, recombinant terminal deoxynucleotidyl transferase (rTdT), RNAase A solution, sodium chloride (NaCl), sodium phosphate monobasic (NaH2PO4), sodium phosphate dibasic (Na2HPO4), tris base, trypan blue and trypsin-Ethylenediaminetetraacetic acid (EDTA) were purchased from Sigma Aldrich (USA). Doxorubicin, cisplatin and vinblastine were obtained from ICN Biomed (USA) while formaldehyde from Carl Roth (Germany) and JC-1 (5, 5´, 6, 6´-tetrachloro-1, 1´, 3 3´-tetraethylbenzimidazol-carbocyanine iodide) from Cayman chemical company (USA). The Plasmid Bolivar and Rodriguez 322 (pBR322) and triton-X-100 were provided by Wako (Japan) while saline sodium citrate (SSC) and fluorescein-12-dUTP by Promega (USA).

### *Collection and Identification of T. patula*

Fresh and uncrushed yellowish orange flowers (5.2 kg) of *T. patula* were collected from the gardens of HEJ Research Institute of Chemistry, University of Karachi. Flowers were identified by plant taxonomist (Dr. Rubina Dawar, Botany Department, University of Karachi, Pakistan) and a voucher specimen (KUH GH No. 67280) was placed in the herbarium of the same department. The patuletin (~2 gm) was obtained by extracting and fractionating the flowers of *T. patula* as reported earlier.[17]

### *Sulforhodamine B (SRB) assay*

The growth inhibition and cytotoxic potential of patuletin was evaluated on human large cell lung carcinoma (NCI-H460) cell line using the protocol described by the National Cancer Institute (NCI), USA.[20] Briefly, the trypsinized NCI-H460 cells were seeded at a density of 7500 cells/well/100 µL in 96-well plates and incubated (24h) in a humidified carbon dioxide ($CO_2$) incubator to obtain a monolayer. Test agents i.e., patuletin (10 - 100 µM), and doxorubicin (0.01, 0.1, 0.5, 5, 10 µM) were added (100 µL/well), followed by incubation for 48h. Afterwards, the cells were fixed using ice-cold trichloroacetic acid (TCA, 50%) followed by staining with SRB (0.4%). The plates were washed with acetic acid (1%) for the removal of unbound SRB stain and were air dried for 12 hours. To solubilize the SRB stain, the Tris base (100 µL of 10 mM) was added, and the plates were kept at plate shaker for 5-10 minutes, followed by optical density (OD) measurement at 515 nm using a spectrophotometer. The growth inhibitory [$GI_{50}$ (50% growth inhibition) and TGI (total growth inhibition)] and cytotoxic [LC50 (50% lethal concentration)] values were obtained graphically as per the description provided by NCI.

### *Cell cycle analysis*

The cell cycle analysis was performed using flow cytometry. Briefly, the NCI-H460 cells were seeded in 6-well plates (1 × 106 cells/well) and incubated (37ºC, 5% $CO_2$)

for 24 hours. Afterwards, various treatments i.e., culture medium (control) or DMSO (0.1%, vehicle control) or patuletin (25, 50 and 100 µM) or doxorubicin (5µM) were given to cells. After 48 hours, cells were washed, trypsinized (500 µL/well) and collected in a micro-centrifuge tube (2 mL). These tubes were centrifuged (2500 rpm, 10 min) to obtain a cell pellet, which was washed thrice with PBS (1 mL) followed by centrifugation (250g, 5 min). The cell suspension was prepared by adding PBS (500 µL) and ice-cold ethanol (100%, 500 µL) under constant vortex and placed at 4ºC overnight. The next day, cells were centrifuged (300g, 1h), treated with RNAase A solution (500 U/mL), and incubated for 30 min. Finally, propidium iodide (25 µg/mL) was added and allowed to stand on ice for 30 min. Cell cycle distribution was analyzed by flow cytometry on a fluorescence-activated cell sorting (FACS) Calibur. Propidium iodide was excited at 488 nm and fluorescence analyzed at 585 nm in FL2-A channel. A total of 20,000 events in each sample were acquired. Using Cellquest Pro software. The percentages of cells at different stages of the cell cycle (i.e., Go/G1, S and G2/M) were determined as described earlier.[20]

***Mitochondrial membrane potential assay***

The mitochondrial membrane potential was evaluated using flow cytometric measurement of JC-1 stain. Briefly, the NCI-H460 cells (1 × 106 cells/mL) were plated in flask (25 cm2) and incubated (5% $CO_2$ at 37 °C) for 24 h to obtain a confluent monolayer. After washing cells with PBS (5 mL), the doxorubicin (5 µM) and patuletin (50 and 100 µM) were added and incubated for 48 h. After trypsinization (1 mL, 0.25%), the fresh medium (RPMI-1640 with 10% FBS) was added and centrifuged (800 rpm for 5min) to obtain the cell pellet. Afterwards, the cells were re-suspended in PBS (1 mL) followed by addition JC-1 stain (0.5 mL, 10 µg/mL) and incubated for 15 mins. After discarding supernatant, the cells were centrifuged twice with PBS (2 mL). Finally, pellet was suspended in PBS (0.5 mL) and examined in flow cytometer (FACS Calibur; Becton Dickinson, USA) using Cell Quest Software. Briefly, the 10,000 cells were counted in triplicate (30,000). The apoptotic cells were shifted from FL-2 to FL-1 region. JC-1-aggregates excitation/emission wavelength was 560/595 nm, while for monomers it was 485/535 nm. The percentage apoptotic index was calculated as follows:

$$\text{Percent apoptotic index} = \frac{\text{Number of apoptotic cells}}{\text{Total number of cells}} \times 100$$

***Transferase dUTP nick end labeling (TUNEL) fluorescence assay***

The NCI-H460 cells (10,000 cells/well) were added in each chamber of 8-well slides and incubated for 24h. Afterwards, the doxorubicin (5 µM) and patuletin (50 and 100 µM) were added to respective wells followed by incubation for 24h. Then, the cells were fixed (4% formaldehyde for 25 minutes at 4°C), permeabilized (0.2% Triton X-100) and equilibrated. The rTdT (50 µL) buffer containing 5 µL nucleotide mix and 1 µL of rTdT (recombinant terminal deoxynucleotidyl transferase) in equilibration buffer was added to each chamber and incubated for 1h in dark humidified chamber. The tailing reaction was stopped by immersing the slide in SSC (2× SSC) buffer for 15 minutes and unincorporated fluorescein-12-dUTP was removed by washing with PBS. The slides were then immersed in propidium iodide solution (1 µg/mL in PBS) for 15 minutes in the dark, washed with deionize water and mounted with 3-4 drops of mounting medium. The photographs of cells were captured using FITC and TxRed filter cubes

attached with a Nikon DXM1200C cooled CCD camera. The images (10×) were captured followed by their real-time de-convolution using NIS-elements 3.0 software (AR version) and processed using Adobe Photoshop software. A total of 1500 cells (500 in triplicate) were counted in both control and treatment having propidium iodide (red color, stains both apoptotic and non-apoptotic cells) and fluorescein-12-dUTP (green color, only apoptotic cells) stains in total cell population. The percent apoptotic index was calculated as follows:

$$\text{Percent apoptotic index} = \frac{\text{Number of apoptotic cells}}{\text{Total number of cells}} \times 100$$

**DNA fragmentation assay**

The DNA fragmentation assay was performed using pBR32 and genomic DNA obtained from NCI-H460 cells. In case of pBR32, the Agarose gel (1%) was prepared in 1x TBE (70 mL), heated in microwave oven (1 min) and allowed to solidify in gel tray at room temperature. The pBR322 (500 ng, 5 µL/well) was mixed with PBS (control), DMSO (0.1%) or patuletin (100 µg/mL) or doxorubicin (100 µg/mL) in a reaction mixture (15 µL) and incubated for 30 min. A mixture of bromophenol blue, xylene cyanol and glycerol (1:1:120, 3 µL/reaction) was added to the above reaction mixture. The sample (18 µL) was applied to the gel and electrophoresis was performed in TBE buffer at 80 V for 1 h. The gels were stained with ethidium bromide solution (5 µg/µL) for 30 minutes followed by de-staining briefly with tap water. The gel was observed under UV Trans-illuminator at 312 nm and the mobility of circular DNA was observed and photographed

In case of genomic DNA, the lysis buffer was added to NCI-H460 cell pellet followed by gentle mixing and placed on ice (15 min). The centrifuged (2000 rpm, 15 min) was performed to obtain the pellet and supernatant was discarded. To the pellet, the nuclear lysis buffer (10 mM Tris-HCl, 400 mM NaCl and 2 mM Na2EDTA, pH 8.2, 2.5 mL), sodium dodecyl sulphate (SDS, 10%, 85 µL) and proteinase K (20 mg/mL, 8 µL) were added and incubated overnight. The saturated sodium chloride solution (6 M, 0.83 mL) was added, vigorously shaken (15 sec) and centrifuged (4000 rpm, 30 min). In fresh tube, the collected supernatant (5 mL) was subjected to ethanol (two volumes) and inverted several times to precipitate DNA. The DNA threads were collected in micro-centrifuge tube (2 mL), washed with ethanol (70%) and left for air-drying (1 h). The Tris-EDTA buffer (250 µL) was added and kept overnight to dissolve DNA. Finally, the electrophoretic mobility assay was performed as described above.

***Gene expression***

The Trizol reagent was used to extract RNA from the aforementioned treated cells followed by assessment of purity using Nanodrop method. Subsequently, the cDNA was synthesized as per manufacturer protocol (Thermo Fisher, USA). The gene expression of BAK, BCL-XL, p53 and GAPDH (housekeeping gene) was assessed by real time PCR (Applied Biosystems, Foster, CA, USA) using gene specific primers (Table 1) and SYBR Green PCR Master Mix. The PCR cycles of each gene consisted of denaturation (94 °C for one minute) followed by thirty-five cycles of amplification with the respective conditions as follows: For BAK and BCL-XL, the annealing was done at 56°C for 1 min, while for p53 and GAPDH, it was 59 °C and 55 °C for 1 min, respectively. However, for all genes, the initial and final extensions were performed at 72 °C for 1 and 10 minutes, respectively.

***Statistical analysis***

The data are expressed as mean ± standard error of mean (S.E.M.) The statistical differences among various means were computed through One-way ANOVA followed by post hoc test (Least significant difference) using SPSS software (v19.0 software, Chicago, IL, USA).

## Results

### *SRB assay*

The growth inhibitory (+) and cytotoxic (-) action of patuletin and doxorubicin against NCI-H460 cell line is shown in Table 2. Patuletin caused dose dependent inhibition of the growth with a $GI_{50}$ of 61 µg/mL. However, at the tested doses (10-100 µM), it failed to completely inhibit the growth (TGI) or demonstrated cytotoxic action ($LC_{50}$). In case of doxorubicin, the $GI_{50}$, TGI and $LC_{50}$ values were found to be 0.26, 3.8 and 9.3 µg/mL respectively.

### *Cell cycle analysis*

The control and vehicle groups revealed that majority of cells were in Go/G1 phase (67%), while S and G2/M phases contains 14% and 19% of cells, respectively (Figure 1). Patuletin treated cells demonstrated a significant concentration dependent increase in Go/G1 phase, while in S phase, a significant increase was noted only at 100 µM dose. However, in G2/M phase, patuletin treated cells exhibited a significant decline leading to complete absence at 100 µM dose. The doxorubicin (5 µM) caused significant increase in Go/G1 and S phases, while G2/M phase was not observed.

### *Mitochondrial membrane potential assay*

The control cells showed the apoptotic index of 5.6%, which was significantly raised to approximately 8% ($P < 0.01$) and 15% ($P < 0.005$) by treatments with patuletin and doxorubicin, respectively (Table 3). The representative plots of these treatments are shown in Figure 2.

### *TUNEL fluorescence assay*

The control cells showed the apoptotic index of 2%, which was significantly raised to 30% ($P < 0.005$) by doxorubicin (Table 4). Similarly, the patuletin treatment also caused significant elevation of apoptotic index to 19% ($P < 0.005$) and 24% ($P < 0.005$) at 50 and 100 µM, respectively. The representative images of these treatments are shown in Figure 3.

### *DNA fragmentation assay*

In case of pBR32, the control and DMSO (1%) treatments exhibit two bands of similar shape with no damaging effect (Figure 4). Likewise, patuletin (100 µg/mL) treatment did not cause any changes in pBR322 DNA band. However, the doxorubicin (100 µg/mL) exposed DNA showed smear formation.

In case of genomic DNA, the control and DMSO group exhibit single healthy band of genomic DNA. Similarly, the patuletin treated DNA was also similar to that of controls. Conversely, doxorubicin treated DNA showed smear formation on the gel.

### *Gene expression*

The patuletin treatment has significantly upregulated the expression of BAK gene in NCI-H460 cells by approximately 50 ($P < 0.05$) and 90 ($P < 0.01$) folds at the tested doses of 25 µM and 50 µM respectively as compared with untreated cells (Figure 5). In case of doxorubicin treatment (5 µM), this increase was found to be 185 folds ($P < 0.005$).

BCL-XL showed approximately 3 ($P < 0.05$) and 16 ($P < 0.005$) folds increase in expression following patuletin and Doxorubicin treatments, respectively.

The expression of p53 gene was mildly upregulated ($P < 0.05$) by patuletin (100 µM) compared with untreated control. However, doxorubicin (0.1 and 1 µM) has significantly increased its expression.

## Discussion

Patuletin arrested the growth of NCI-H460 cells. The cell cycle analysis revealed significant increase in $G_o/G_1$ and S phases, while $G_2$/M phase was found to be declined. The apoptotic index exhibited significant elevation, while no effect on the structure of DNA was observed. The expression data revealed alterations in all tested genes but BAK exhibited remarkable upregulation. The overall data showed that patuletin caused growth inhibition of NCI-H460 via the induction of BAK-mediated apoptosis.

SRB assay, due to high efficiency and cost effectiveness, is the most common screening method for assessment of anti-cancer activity.[21] Using this assay, patuletin exhibited the $GI_{50}$ value of 61 µg/mL (Table 2). However, it failed to cause cytotoxicity at the tested doses of 10 - 100 µM. Patuletin is a major flavonoid in Tagetes flower with structural attributes (C2–C3 unsaturation and 3-hydroxyl groups and methoxy group at C6 position) supporting anti-proliferative action.[19] Keeping this into account, the cell cycle analysis was performed to further confirm its effect on cellular proliferation. The data showed that patuletin treatment caused significant increase in the frequency of cells in both Go/G1 and S phases, which is suggestive of cell cycle arrest in these phases (Figure 1). Thus, it further supports the notion is patuletin is endowed with the ability to arrest growth of NCI-H460 cells.

Apoptosis, the programmed cell death, is an important pharmacological target of anti-cancer drugs.[22] Therefore, the apoptotic index of cells was assessed following treatment with patuletin. In this regard, the mitochondrial membrane potential was evaluated as an early indicator of apoptosis.[23] In conformity with literature, the doxorubicin treatment has significantly raised the apoptotic index in NCI-H460 cells, thereby supporting the methodology [24]. The data further revealed significant increase in the apoptotic index following treatment with patuletin (Table 3 and Figure 2). This suggest that the growth arrest of NCI-H460 was most likely due to induction of apoptosis. Literature also suggests the initiation of apoptosis as the primary mechanism of anticancer action by flavonoids.[25] In order to further confirm apoptosis as the underlying cause of anti-cancer action demonstrated by patuletin, the TUNEL fluorescence method was used. This assay is considered as a reporter assay for later stages of apoptosis.[26] It is of note that the enhanced apoptotic index was also observed in this assay. Thus, it further validates that the induction of apoptosis is the most likely mode of anticancer action by patuletin (Table 4 and Figure 3).

DNA damaging chemotherapies are also used to treat cancer such as doxorubicin.[27] Therefore, the effect of patuletin on the structural integrity of both plasmid and genomic DNA was investigated. In conformity with existing literature, the doxorubicin caused smear formation in both types of DNA, which is indicative of strand breaks or fragmentation (Figure 4). However, the patuletin treated DNA was similar to that of controls. This suggests lack of the involvement of DNA in exhibiting its anticancer action.

The pathogenesis as well as treatment of cancer is often governed by the expression of several genes. Keeping this into account, the expression of three genes of interest were also studied. Two of the genes belongs to Bcl-family i.e., BAK and BCL-XL. The BAK gene is pro-apoptotic in nature,[28] while BCL-XL is known to inhibit the phenomenon of apoptosis.[29] Another gene under study was p53, named as tumor suppressor gene because it regulates the cell division in a manner to avoid too fast and uncontrolled proliferation.[30] Although, the patuletin treatment enhanced the expression of all genes, but the remarkable effect was noted only in BAK gene (Figure 5). The

significantly enhanced expression of this pro-apoptotic gene further supports previously mentioned deduction regarding induction of apoptosis as most likely mechanism of anticancer action by patuletin. In similar lines, literature also suggest the upregulation of pro-apoptotic genes by the flavonoids.[31] Literature revealed that the p53 gene-mediated apoptosis is attributed to DNA stand breaks,[32] which was not observed in earlier study. Thus, the lack of obvious change in p53 expression also retrospectively supports the outcome of DNA fragmentation assay.

The present study demonstrates that Patuletin, the major flavonoid in *Tagetes patula* flower, is endowed with the potential to arrest the growth of non-small cell lung cancer. The most likely cause of this effect is the induction of apoptosis. Therefore, the compound presents itself as a promising candidate for small-cell lung cancer drug discovery program.

The main limitations of the study are the use of single cancer cell lines. The ability of patuletin to differentiate between normal and cancerous cells was not evaluated. Additionally, the in-vivo effectiveness of the compound is yet to be assessed in animal model of lung cancer.

**Acknowledgements**
None declared.

**Authors' Contributions**
SI: Data acquisition; data analysis and interpretation; drafting and reviewing of the manuscript.
HK, AK, MAUK, AR, MA, TR and SF: Data acquisition; data analysis and interpretation
ADF and MK: Study design and critical reviewing of manuscript. All authors have read and approved the final manuscript and agreed to be accountable for all aspects of the work in ensuring that questions related to the accuracy or integrity of any part of the work are appropriately investigated and resolved.

**Funding**
None declared.

**Conflict of Interest**
The authors declare that the study was conducted in the absence of any commercial or financial relationships that could be construed as a potential conflict of interest.

**References**

1. Mattiuzzi C, Lippi G. Current cancer epidemiology. *J Epidemiol Glob Health.* 2019;9(4):217-22. doi: 10.2991/jegh.k.191008.001. PMID: 31854162; PMCID: PMC7310786.
2. Thandra KC, Barsouk A, Saginala K, Aluru JS, Barsouk A. Epidemiology of lung cancer. *Contemp Oncol (Pozn).* 2021;25(1):45-52. doi: 10.5114/wo.2021.103829. PMID: 33911981; PMCID: PMC8063897.
3. Bray F, Ferlay J, Soerjomataram I, Siegel RL, Torre LA, Jemal A. Global cancer statistics 2018: GLOBOCAN estimates of incidence and mortality worldwide for 36 cancers in 185 countries. *CA Cancer J Clin.* 2018;68(6):394-424. doi: 10.3322/caac.21492. Erratum in: *CA Cancer J Clin.* 2020;70(4):313. doi: 10.3322/caac.21609. PMID: 30207593.
4. Travis WD, Brambilla E, Nicholson AG, Yatabe Y, Austin JHM, Beasley MB, et al. The 2015 World Health Organization classification of lung tumors: Impact of genetic, clinical and radiologic advances since the 2004 classification. *J Thorac Oncol.* 2015;10(9):1243-60. doi: 10.1097/JTO.0000000000000630. PMID: 26291008.
5. Sheikh HS, Munawar K, Sheikh F, Qamar MFU. Lung cancer in Pakistan. *J Thorac Oncol*. 2022;17(5):602-7.

doi: 10.1016/j.jtho.2022.01.009. PMID: 35465966.
6. Alexander M, Kim SY, Cheng H. Update 2020: management of non-small cell lung cancer. *Lung*. 2020;198(6):897-907. doi: 10.1007/s00408-020-00407-5. PMID: 33175991; PMCID: PMC7656891.
7. Lin A, Wei T, Meng H, Luo P, Zhang J. Role of the dynamic tumor microenvironment in controversies regarding immune checkpoint inhibitors for the treatment of non-small cell lung cancer (NSCLC) with EGFR mutations. *Mol Cancer*. 2019;18(1):139. doi: 10.1186/s12943-019-1062-7. PMID: 31526368; PMCID: PMC6745418.
8. Cragg GM, Grothaus PG, Newman DJ. Impact of natural products on developing new anti-cancer agents. *Chem Rev*. 2009;109(7):3012-43. doi: 10.1021/cr900019j. PMID: 19422222; PMCID: PMC2752977.
9. Chattopadhyay S, Sarkar SS, Saproo S, Yadav S, Antil D, Das B, et al. Apoptosis-targeted gene therapy for non-small cell lung cancer using chitosan-poly-lactic-co-glycolic acid-based nano-delivery system and CASP8 and miRs 29A-B1 and 34A. *Front Bioeng Biotechnol*. 2023;11:1188652. doi: 10.3389/fbioe.2023.1188652. PMID: 37484755; PMCID: PMC10360353.
10. Neely V, Manchikalapudi A, Nguyen K, Dalton K, Hu B, Koblinski JE, et al. Targeting oncogenic mutant p53 and BCL-2 for small cell lung cancer treatment. *Int J Mol Sci*. 2023;24(16):13082. doi: 10.3390/ijms241613082. PMID: 37629205; PMCID: PMC10455832.
11. Park D, Anisuzzaman ASM, Magis AT, Chen G, Xie M, Zhang G, et al. Discovery of small molecule Bak activator for lung cancer therapy. *Theranostics*. 2021;11(17):8500-16. doi: 10.7150/thno.59223. PMID: 34413615; PMCID: PMC8370720.
12. Chitrakar B, Zhang M, Bhandari B. Edible flowers with the common name "marigold": Their therapeutic values and processing. *Trends Food Sci Technol*. 2019;89:76-87. doi: 10.1016/j.tifs.2019.05.008.
13. Faizi S, Siddiqi H, Bano S, Naz A, Lubna Mazhar K, Nasim S, et al. Antibacterial and antifungal activities of different parts of Tagetes patula: preparation of patuletin derivatives. *Pharm Biol*. 2008;46(5):309-20. doi: 10.1080/13880200801982867. PMID: 18686128.
14. Jabeen A, Mesaik MA, Simjee SU, Bano S, Faizi S. Anti-TNF-α and anti-arthritic effect of patuletin: A rare flavonoid from Tagetes patula. *Int Immunopharmacol*. 2016;36:232-40. doi: 10.1016/j.intimp.2016.05.003. PMID: 27208629.
15. Azeemi K. Rang-o-Roshni se Ilaj. Karachi: Al-Kitab Publications; 1999. p.42-43.
16. Zheng J, Lu B, Xu B. An update on the health benefits promoted by edible flowers and involved mechanisms. *Food Chem*. 2021;340:127940. doi: 10.1016/j.foodchem.2020.127940. PMID: 32987120.
17. Kashif M, Bano S, Naqvi S, Faizi S, Lubna, Ahmed Mesaik M, et al. Cytotoxic and antioxidant properties of phenolic compounds from Tagetes patula flower. *Pharm Biol*. 2015;53(5):672-81. doi: 10.3109/13880209.2014.931441. PMID: 25124078.
18. Zhu W, Lv C, Wang J, Gao Q, Zhu H, Wen H. Patuletin induces apoptosis of human breast cancer SK-BR-3 cell line via inhibiting fatty acid synthase gene expression and activity. *Oncol Lett*. 2017;14(6):7449-54. doi: 10.3892/ol.2017.7113. PMID: 29250198; PMCID: PMC5726893.

19. Alvarado-Sansininea JJ, Sánchez-Sánchez L, López-Muñoz H, Escobar ML, Flores-Guzmán F, Tavera-Hernández R, et al. Quercetagetin and patuletin: antiproliferative, necrotic and apoptotic activity in tumor cell lines. *Molecules*. 2018;23(10):2579. doi: 10.3390/molecules23102579. PMID: 30301137; PMCID: PMC6225169.
20. Skehan P, Storeng R, Scudiero D, Monks A, McMahon J, Vistica D, et al. New colorimetric cytotoxicity assay for anticancer-drug screening. *J Natl Cancer Inst*. 1990;82(13):1107-12. doi: 10.1093/jnci/82.13.1107. PMID: 2359136.
21. Vichai V, Kirtikara K. Sulforhodamine B colorimetric assay for cytotoxicity screening. *Nat Protoc*. 2006;1(3):1112-6. doi: 10.1038/nprot.2006.179. PMID: 17406391.
22. Pfeffer CM, Singh AT. Apoptosis: a target for anticancer therapy. *Int J Mol Sci*. 2018;19(2):448. doi: 10.3390/ijms19020448. PMID: 29393886; PMCID: PMC5855679.
23. Sivandzade F, Bhalerao A, Cucullo L. Analysis of mitochondrial membrane potential using JC-1 dye. *Bio Protoc*. 2019;9(1):e3128. doi: 10.21769/BioProtoc.3128. PMID: 35083633; PMCID: PMC8782320.
24. Mizutani H, Tada-Oikawa S, Hiraku Y, Kojima M, Kawanishi S. Mechanism of apoptosis induced by doxorubicin through generation of hydrogen peroxide. *Life Sci*. 2005;76(13):1439-53. doi: 10.1016/j.lfs.2004.10.040. PMID: 15680305.
25. Ponte LGS, Pavan ICB, Mancini MCS, da Silva LGS, Morelli AP, Severino MB, et al. The hallmarks of flavonoids in cancer. *Molecules*. 2021;26(7):2029. doi: 10.3390/molecules26072029. PMID: 33805093; PMCID: PMC8037345.
26. yrylkova K, Kyryachenko S, Leid M, Kioussi C. Detection of apoptosis by TUNEL assay. *Methods Mol Biol*. 2012;887:41-7. doi: 10.1007/978-1-61779-860-3_5. PMID: 22610562.
27. van der Zanden SY, Qiao X, Neefjes J. New insights into activities and toxicities of doxorubicin. *FEBS J*. 2021;288(21):6095-111. doi: 10.1111/febs.15519. PMID: 33006134; PMCID: PMC8513754.
28. lrich E, Kauffmann-Zeh A, Hueber AO, Williamson J, Chittenden T, Ma A, et al. Gene structure, cDNA sequence, and expression of murine Bak. *Genomics*. 1997;44(2):195-200. doi: 10.1006/geno.1997.4847. PMID: 9325044.
29. Li M, Wang D, He J, Chen L, Li H. Bcl-XL: A multifunctional anti-apoptotic protein. *Pharmacol Res*. 2020;151:104547. doi: 10.1016/j.phrs.2019.104547. PMID: 31705974.
30. assin O, Oren M. Drugging p53 in cancer: one protein, many targets. *Nat Rev Drug Discov*. 2023;22(2):127-44. doi: 10.1038/s41573-022-00571-8. PMID: 36307504.
31. Chand P, Kumar H, Jain R, Jain A, Jain V. Flavonoids as omnipotent candidates for cancer management. *S Afr J Bot*. 2023;158:334-46. doi: 10.1016/j.sajb.2023.04.016.
32. Pellegata NS, Antoniono RJ, Redpath JL, Stanbridge EJ. DNA damage and p53-mediated cell cycle arrest: a reevaluation. *Proc Natl Acad Sci U S A*. 1996;93(26):15209-14. doi: 10.1073/pnas.93.26.15209. PMID: 8986799; PMCID: PMC26386.

Table 1. Primers sequences of the genes of interest

| Gene | Primer sequence |
|---|---|
| BAK | F-GGTCCTGCTCAACTCTACCC |
| | R-CCTGAGAGTCCAACTGCAAA |
| BCL-XL | F-GGCATTCAGTGACCTGACATC |
| | R-AGTCATGCCCGTCAGGAAC |
| p53 | F-GCCCAACAACACCAGCTCCT |
| | R-CCTGGGCATCCTTGAGTTCC |
| GAPDH | F-GGAAAGCTGTGGCGTGATGG |
| | R-GTAGGCCATGAGGTCCACCA |

The significant difference is marked with the asterisk sign with following confidence of interval; BAK: Bcl-2 homologous antagonist/killer; BCL-XL: B-cell lymphoma-extra large; GAPDH: Glyceraldehyde-3-phosphate dehydrogenase

Table 2. Growth inhibitory and cytotoxic actions of patuletin against the NCI-H460 cell line

| Treatments | Doses (μM) | Growth inhibition / cytotoxicity | $GI_{50}$ | TGI | $LC_{50}$ |
|---|---|---|---|---|---|
| | | | (μg/mL) | | |
| **NCI-H460 cell line** | | | | | |
| Patuletin | 10.00 | +1.00 ± 1.00 | 61.00 | ND | ND |
| | 20.00 | +10.00 ± 9.00* | | | |
| | 25.00 | +18.00 ± 8.00** | | | |
| | 50.00 | +40.00 ± 3.00*** | | | |
| | 100.00 | +82.00 ± 2.00*** | | | |
| Doxorubicin | 0.01 | +1.00 ± 1.00 | 0.26 | 3.80 | 9.30 |
| | 0.10 | +37.00 ± 9.00** | | | |
| | 0.50 | +81.00 ± 8.00*** | | | |
| | 5.00 | –27.00 ± 3.00*** | | | |
| | 10.00 | –54.00 ± 2.00*** | | | |

ND: Not detected at tested dose range; Asterisks indicate the level of significance as follows: * ($P < 0.05$), ** ($P < 0.01$) and *** ($P < 0.005$); $GI_{50}$: Growth inhibition 50%; TGI: Total growth inhibition; $LC_{50}$: Lethal concentration 50%; NCI-H460: National Cancer Institute - Human non-small cell lung cancer 460

Table 3. Apoptotic effects of patuletin against NCI-H460 cell line using MMP Assay

| Treatment | Dose (µM) | Apoptotic cells (count) | Apoptotic index (%) |
|---|---|---|---|
| Patuletin | 50.00 | 875.00 ± 22.00** | 8.80 |
| | 100.00 | 773.00 ± 12.00** | 7.70 |
| Doxorubicin | 5.00 | 1489.00 ± 21.00*** | 15.00 |
| Control | - | 560.00 ± 60.00 | 5.60 |

Asterisks indicate the level of significance as follows: ** ($P < 0.01$) and *** ($P < 0.005$) as compared with control; MMP: Mitochondrial membrane potential; NCI-H460: National Cancer Institute - Human non-small cell lung cancer 460

Table 4. Apoptotic effects of patuletin against NCI-H460 cell line using TUNEL Assay

| Treatment | Dose (µM) | Apoptotic cells (count) | Apoptotic index (%) |
|---|---|---|---|
| **Patuletin** | 50.00 | 95.00 ± 3.80*** | 19.00 |
| | 100.00 | 120.00 ± 7.60*** | 24.00 |
| **Doxorubicin** | 5.00 | 150.00 ± 12.00*** | 30.00 |
| **Control** | - | 10.00 ± 1.00 | 2.00 |

Asterisks indicate the level of significance as follows: *** ($P < 0.005$) as compared with control; TUNEL: Terminal deoxynucleotidyl transferase dUTP nick end labeling; NCI-H460: National Cancer Institute - Human non-small cell lung cancer 460

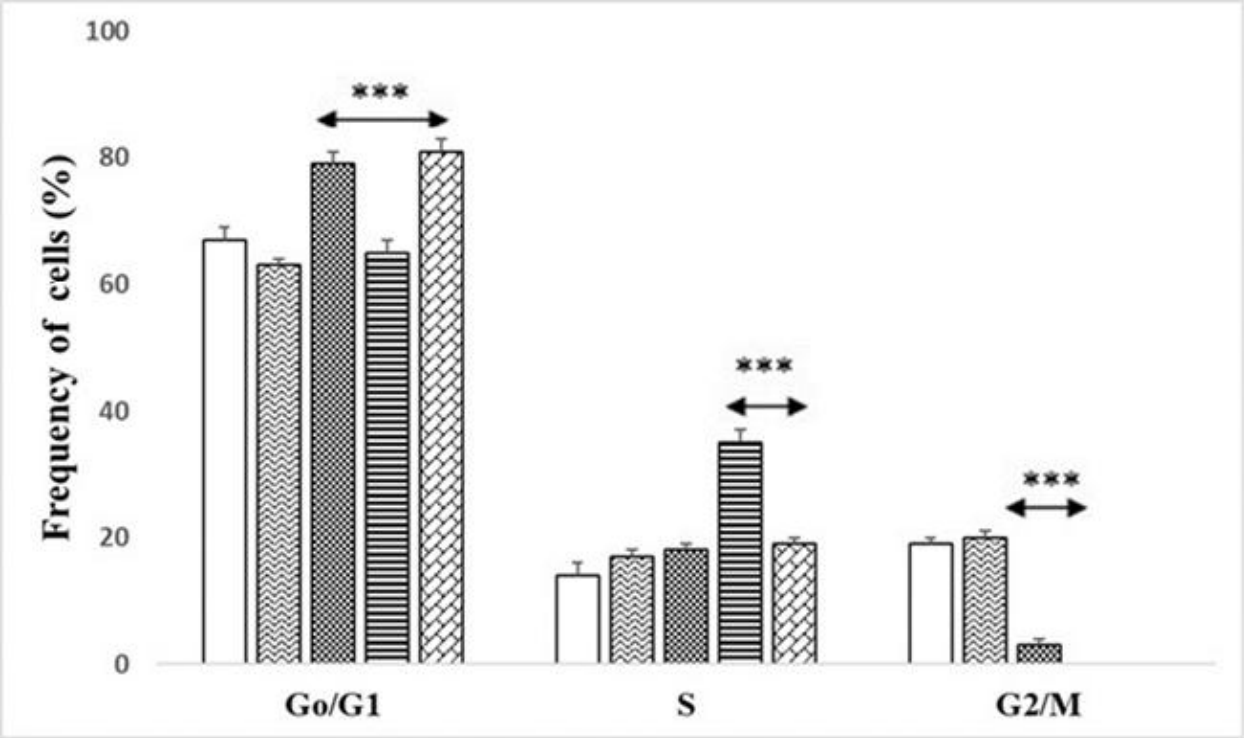


Figure 1. Effect of patuletin on the various phases of cell cycle: The figure exhibits the effect on various phases ($G_o$/GI, S and G2/M) of cell cycle following treatment with control (□), patuletin [25 (▨), 50 (▩) and 100 (▤) µM] and doxorubicin (5 µM,▨). The control cells were mostly in $G_o$/GI phase, which was further raised by both patuletin and doxorubicin. Similar effect of both agents was observed in case of S phase. However, the opposite effect was noted in case of G2/M phase, whereby the cell frequency was significantly suppressed to zero by both patuletin and doxorubicin. The data is presented as mean ± SEM of frequency on cell in various phases of cell cycle. Asterisk ($P < 0.005$) indicate the statistical difference as compared to control

SEM: Standard error of mean; Go/G1: Resting phase/Gap 1; S: Synthesis phase; G2/M: Gap 2/Mitotic phase

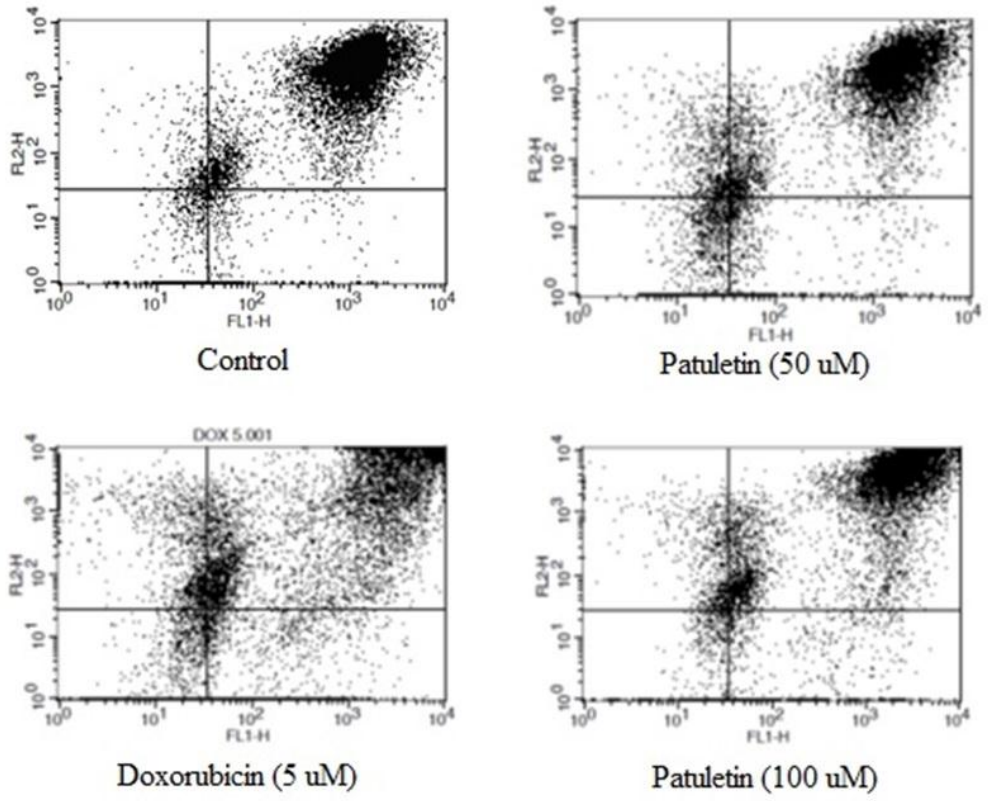


Figure 2. Representative flow cytometry plots of various treatments using JC-1 stain: The figure depicts the representative plots of control NCI-H460 cells and the ones treated with doxorubicin and patuletin. The apoptotic action is marked with shift of cells from FL2-H to FL1-H. The patuletin treatment (50 and 100 uM) caused significant shift from FL2-H to FL1-H, which was found to be more obvious in case of treatment with doxorubicin. A total of 10,000 cells were counted in triplicate against each treatment.

JC-1: 5, 5´, 6, 6´- tetrachloro-1, 1´, 3 3´- tetraethylbenzimidazol-carbocyanine iodide; FL2-H: Fluorescence channel 2- height; FL1-H: Fluorescence channel 1- height

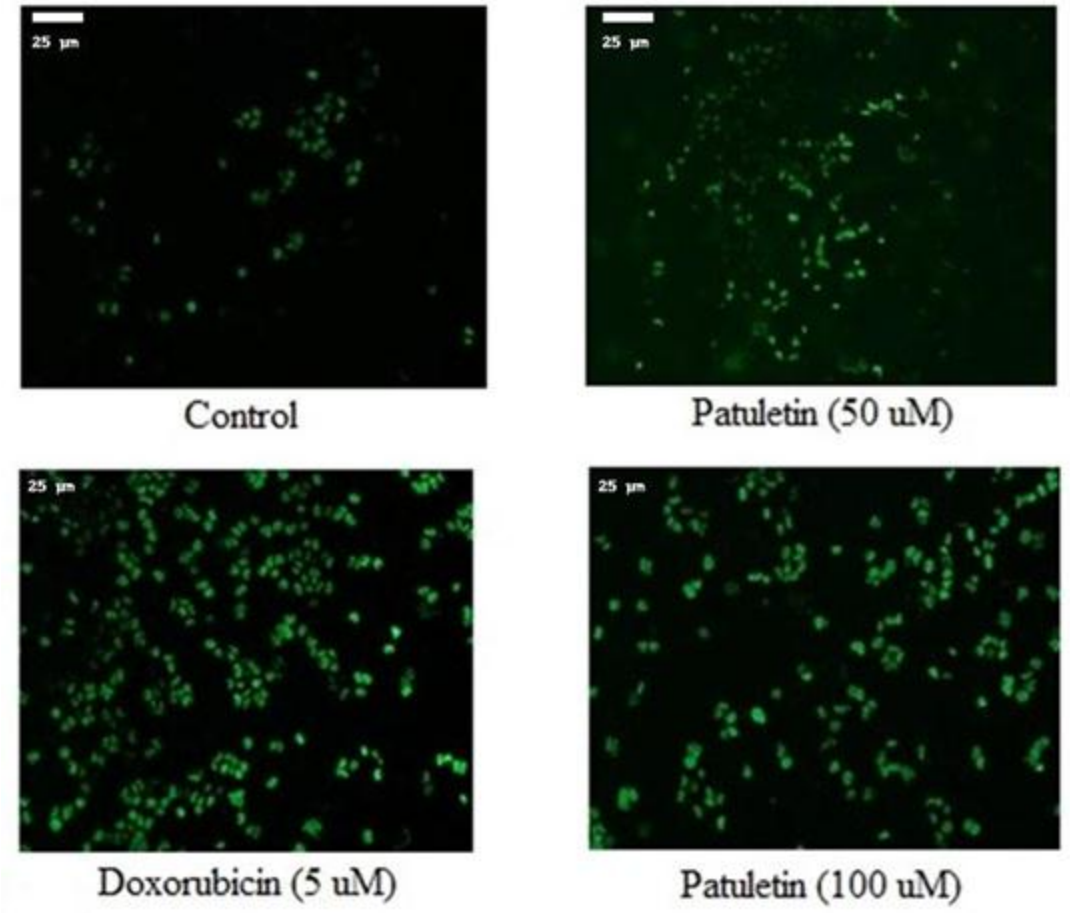


Figure 3. Representative images of various treatments using TUNEL assay: The figure exhibit the representative fluorescence images of control NCI-H460 cells and the ones treated doxorubicin (5 uM) and patuletin (50 and 100 uM). The marked increase in the green fluorescence indicative of apoptotic action can be observed in case of both standard and test drugs as compared with control.

TUNEL: Terminal deoxynucleotidyl transferase dUTP nick end labeling; NCI-H460: National Cancer Institute - Human non-small cell lung cancer 460

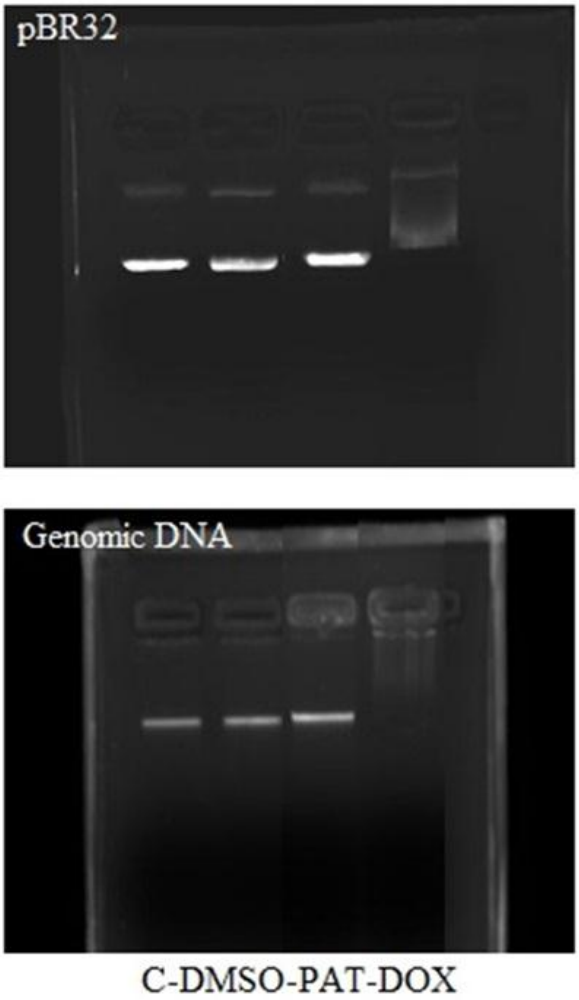


Figure 4. Effect of Patuletin on fragmentation of pBR32 and genomic DNA: The figure depicts the effect of various treatment on electrophoretic mobility shift of DNA. The control (C), vehicle control (0.1% DMSO) and patuletin (PAT, 100 µg/mL) doses not exhibit any effect on both types of DNAs. However, the smear formation was noted following treatment with doxorubicin (DOX, 100 µg/mL). The figure is prepared by cropping the required data from original gel images provided in the supplementary files.

C: Control; DMSO: Dimethyl sulfoxide; PAT: Patuletin; DOX: Doxorubicin

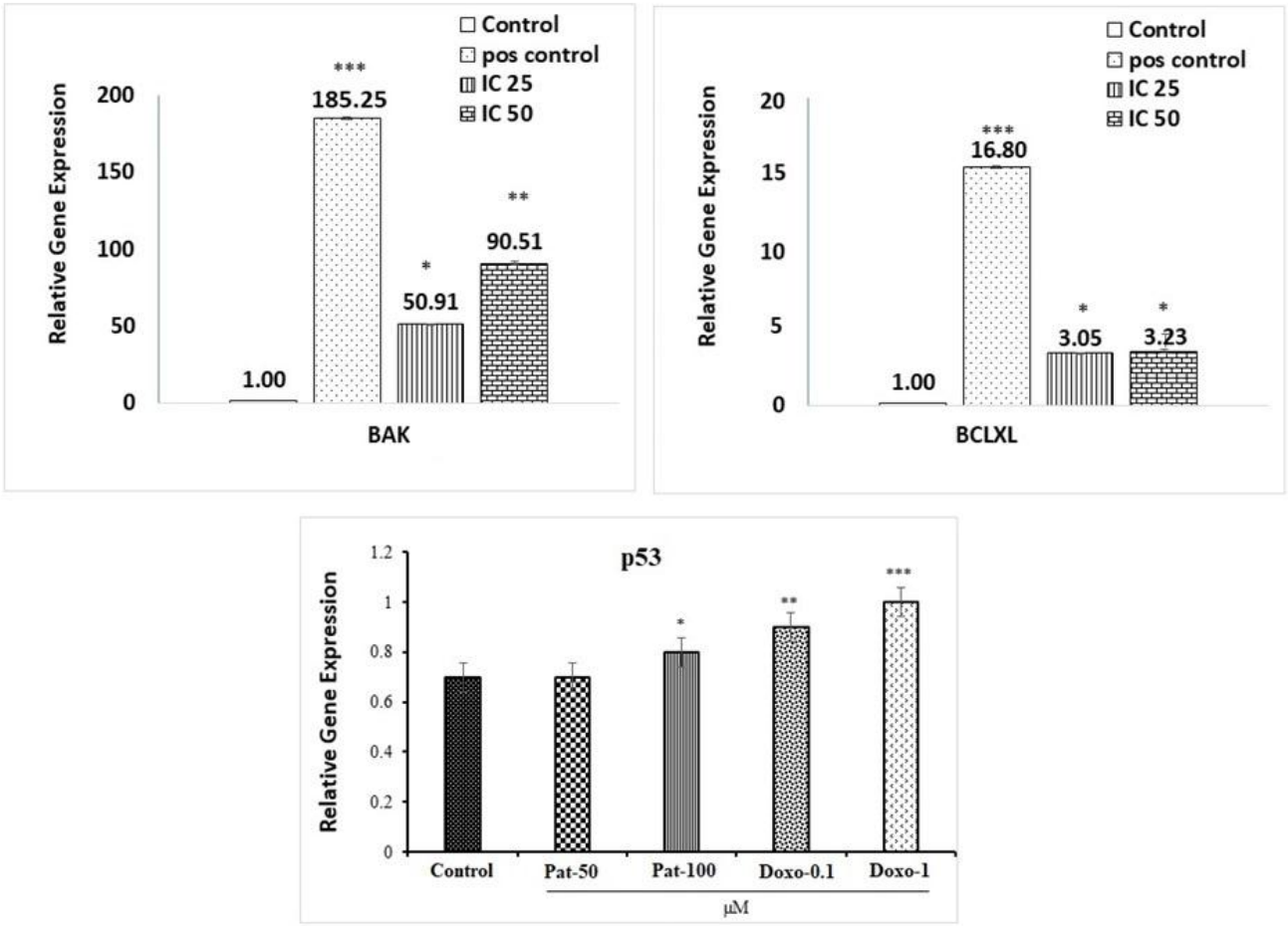


Figure 5. Effect of patuletin on expression of BAK, BCL-XL and p53 genes: The figure depicts the effect of patuletin treatment on the pro-apoptotic (BAK), anti-apoptotic (BCL-XL) and tumor suppressor (p53) genes of NCI-H460 cells. The patuletin appeared to have significant effect on the upregulation of BAK gene, which was also noted in case of treatment with doxorubicin. In case of BCL-XL and p53 genes, the effect of patuletin was negligible. In comparison, the doxorubicin shows the comparatively higher upregulation of these genes but it is trivial as compared with its effect on BAK gene.

Asterisks indicate the level of significance as follows: $^{*}$ ($P < 0.05$), $^{**}$ ($P < 0.01$) and $^{***}$ ($P < 0.005$) as compared with control; BAK: Bcl-2 homologous antagonist/killer; BCL-XL: B-cell lymphoma-extra large; NCI-H460: National Cancer Institute - Human non-small cell lung cancer 460